PROCEEDINGS OF SCIENCE

Mixing and CP violation in the decay $B_s \rightarrow J/\psi\phi$ in ATLAS

William James Dearnaley*Lancaster University

E-mail: william.james.dearnaley@cern.ch

A measurement of the $B_s^0 \rightarrow J/\psi\phi$ decay parameters, updated to include flavour tagging, is reported using 4.9 fb^{-1} of integrated luminosity collected by the ATLAS detector from pp collisions recorded in 2011. A search for new physics was undertaken by measuring the weak phase ϕ_s, the mean lifetime Γ_s and the lifetime difference $\Delta\Gamma_s$.

The 15th International Conference on B-Physics at Frontier Machines at the University of Edinburgh
14 -18 July, 2014
University of Edinburgh, UK

*Speaker.

1. Introduction

ATLAS is a multi-purpose detector, built to study a vast array of particle physics processes. ATLAS has a precision outer Muon Spectrometer (MS) for $|\eta| < 2.5$, with resolution $\sim$40 μm per measurement and an Inner Detector (ID) for $|\eta| < 2.5$ with resolution $\sim$10 μm per measurement.

Tagging has been added to the analysis of the 2011 ATLAS data. This allows for an estimate of the charge of the b within the B_s^0 candidate. This has been done with muon and jet tags, calibrated on $B^\pm \to J/\psi K^\pm$ events.

2. Data Selection

Data were collected during a period of rising instantaneous luminosity, with the trigger conditions varying over time.

- Selection triggers are based on identification of a $J/\psi \to \mu^+\mu^-$ decay with two 4 GeV p_T thresholds, or asymmetric p_T thresholds with one muon at e.g. above a 4 GeV p_T threshold and a second muon with p_T above 2 GeV.
- More than one primary vertex is required, formed from ≥ 4 ID tracks, and ≥ 2 oppositely charged muon candidates reconstructed using MS and ID information. The muon pair invariant mass is calculated from the refitted track parameters, with different acceptance windows for muons both within the barrel, both within end-cap, or one in each region; the mass window is defined so as to accept 99.8% of the events.
- $\phi \to K^+K^-$ candidates are reconstructed from all pairs of oppositely charged particles with $p_T > 0.5$ GeV and $|\eta| < 2.5$ that are not identified as muons.
- A cut is applied to the vertex quality of the B_s^0 reconstructed from the two muon and two kaon tracks. This vertex must have χ^2 / d.o.f.< 3.

3. Tagging

A charge tag is defined for both muons and jets as in equation 3.1.

$$Q_{\mu,jet} = \frac{\sum_i^{N_{tracks}} q^i \cdot (p_T^i)^k}{\sum_i^{N_{tracks}} (p_T^i)^k} \tag{3.1}$$

where the value of the parameter k = 1.1, which was tuned to optimise the tagging power for this analysis. For muons, the sum is performed over the reconstructed ID tracks within a cone of opening angle ΔR< 0.5 around the muon momentum axis, with $p_T > 0.5$ GeV and $|\eta| < 2.5$. For jets the sum is over the tracks associated to the jet.

Differences in the distributions of the tagging probability between the signal and background is accounted for through the addition of new terms in the likelihood function. The tagging methods are calibrated on $B^\pm \to J/\psi K^\pm$ events, as the b-parton charge is known at production, given by the final state. Figure 1 demonstrates the performance of each tagging method in the final data sample used. Table 1 shows the efficiency, dilution and tagging power of the three tagging methods.

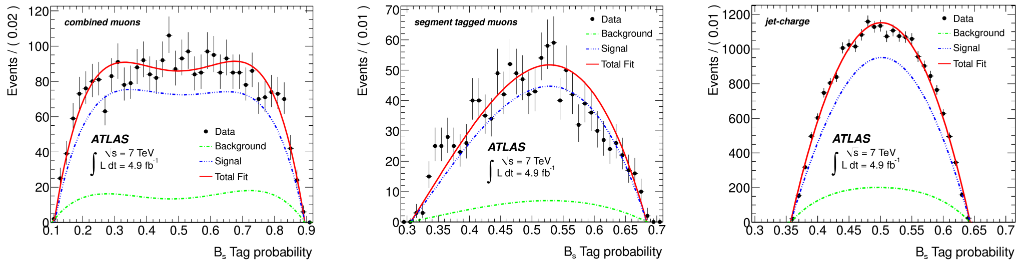

(a) Combined muons (b) Segment tagged muons (c) Jet-charge

Figure 1: The tag probability for tagging using (a) combined muons, (b) segment tagged muons, (c) jet-charge. Black dots are data, blue is a fit to the sidebands, green to the signal and red is a sum of both fits (taken from [1]).

Table 1: Efficiency, dilution and tagging power of the three tagging methods used.

Tagger	Efficiency [%]	Dilution [%]	Tagging Power [%]
Combined μ	3.37 ± 0.04	50.6 ± 0.5	0.86 ± 0.04
Segment Tagged μ	1.08 ± 0.02	36.7 ± 0.7	0.15 ± 0.02
Jet Charge	27.7 ± 0.1	12.68 ± 0.06	0.45 ± 0.03
Total	32.1 ± 0.1	21.3 ± 0.08	1.45 ± 0.05

4. Fit Method

An unbinned maximum likelihood fit to the reconstructed B_s^0 mass, proper decay time and transversity angles is performed to extract the lifetime of the B_s^0 meson. Many sources contribute to the background. The mass and proper decay time are simultaneously fitted using the likelihood function in equation 4.1.

$$\ln \mathscr{L} = \sum_{i=1}^{N} \Big(\ln(f_s \cdot \mathscr{F}_s(m_i, t_i, \Omega_i) + f_s \cdot f_{B^0} \cdot \mathscr{F}_{B^0}(m_i, t_i, \Omega_i) \\ + (1 - f_s \cdot (1 + f_{B^0}))\mathscr{F}_{\mathrm{bkg}}(m_i, t_i, \Omega_i)) \Big) \tag{4.1}$$

where,

- N = number of selected events,
- f_s = fraction of signal candidates,
- f_{B^0} = fraction of B^0 ($B^0 \to J/\psi K^{0*}$ and $B^0 \to J/\psi K^{\pm}\pi^{\pm}$) mesons misidentified as B_s^0, fixed in the fit,
- mass (m_i), proper decay time (t_i), decay angle (Ω_i) are measured for each event i,

- $\mathscr{F}_s$, $\mathscr{F}_{B^0}$, $\mathscr{F}_{bkg}$ = Probability Density Functions for the signal $B_s^0 \to J/\psi\phi$ and the $B_s^0 \to J/\psi K^*$ and combinatorial backgrounds ($bb \to J/\psi X$ and $pp \to J/\psi X$) respectively.

The input variables to the maximum likelihood fit extracted from data are the proper decay time τ_i, its uncertainty σ_{τ_i}, the mass m_i and its uncertainty σ_{m_i}, and the transversity angles θ_i, ϕ_i, and ψ_i, for each B_s^0 candidate passing the selections. Fit projections are shown in Figures 2 and 3.

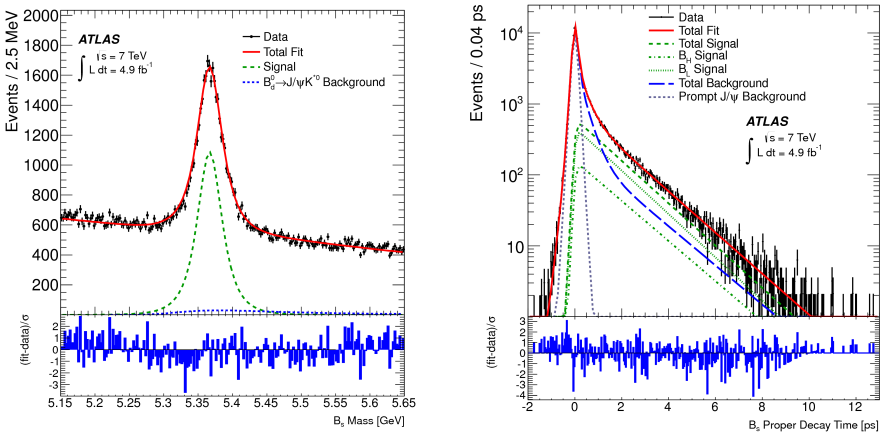

(a) Mass fit projection (b) Proper decay time fit projection

Figure 2: (a) Mass fit projection for the B_s^0. The red line shows the total fit, the dashed green line shows the signal component while the dotted blue line shows the contribution from $B^0 \to J/\phi K^0$ events. The pull distribution at the bottom shows the difference between data and fit value normalized to the data uncertainty (taken from [1]). (b) Proper decay time fit projection for the B_s^0. The red line shows the total fit while the green dashed line shows the total signal. The light and heavy components of the signal are shown as green dotted and a dash-dotted line respectively. The total background is shown as a blue dashed line with a grey dotted line showing the prompt J/ψ background. The pull distribution at the bottom shows the difference between data and fit value normalized to the data uncertainty (taken from [1]).

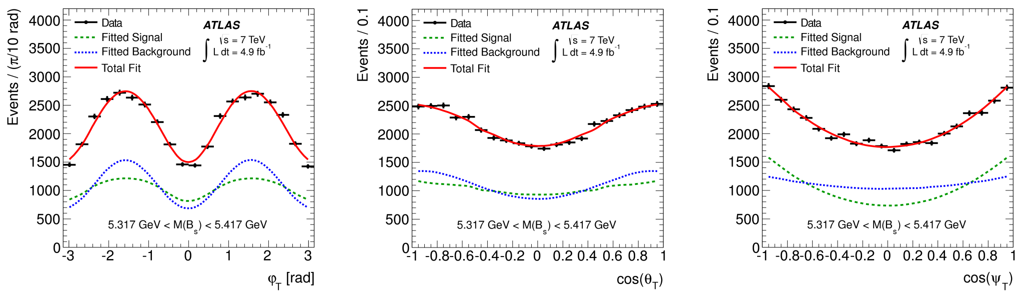

(a) ϕ_T (b) $\cos(\theta_T)$ (c) $\cos(\psi_T)$

Figure 3: Fit projections for the transversity angle (a) ϕ_T, (b) $\cos(\theta_T)$, (c) $\cos(\psi_T)$. The red line shows the total fit, the dashed green line shows the signal component and the dotted blue line shows the background contribution (taken from [1]).

5. Results

The number of signal B_s^0 meson candidates extracted from the fit is 22670 ± 150. The fit results and systematic uncertainties for the measured physics parameters of the simultaneous unbinned maximum likelihood fit are shown in Table 2. A summary of the systematic uncertainties assigned to parameters of interest is presented in Table 3.

Table 2: Results of maximum likelihood fit.

Parameter		Measured Value
CP violating phase	$\phi_s =$	$0.12 \pm 0.25 \pm 0.05$ rad
Lifetime difference	$\Delta\Gamma_s =$	$0.053 \pm 0.021 \pm 0.010$ ps^{-1}
Lifetime	$\Gamma_s =$	$0.677 \pm 0.007 \pm 0.004$ ps^{-1}
S-wave amplitude	$\lvert A_{\parallel}(0)\rvert^2 =$	$0.220 \pm 0.008 \pm 0.009$
CP even component amplitude	$\lvert A_0(0)\rvert^2 =$	$0.529 \pm 0.006 \pm 0.012$
Strong phase angle	$\delta_\perp =$	$3.89 \pm 0.47 \pm 0.11$ rad

Table 3: Summary of systematic uncertainties assigned to parameters of interest.

	ϕ_s (rad)	$\Delta\Gamma_s$ (ps^{-1})	Γ_s (ps^{-1})	$\lvert A_{\parallel}(0)\rvert^2$	$\lvert A_0(0)\rvert^2$	$\lvert A_s(0)\rvert^2$	$\delta_\perp$ (rad)	$\delta_{\parallel}$ (rad)	$\delta_\perp - \delta_s$ (rad)
ID alignment	$< 10^{-2}$	$< 10^{-3}$	$< 10^{-3}$	$< 10^{-3}$	$< 10^{-3}$	–	$< 10^{-2}$	$< 10^{-2}$	–
Trigger efficiency	$< 10^{-2}$	$< 10^{-3}$	0.002	$< 10^{-3}$	$< 10^{-3}$	$< 10^{-3}$	$< 10^{-2}$	$< 10^{-2}$	$< 10^{-2}$
B^0 contribution	0.03	0.001	$< 10^{-3}$	$< 10^{-3}$	0.005	0.001	0.02	$< 10^{-2}$	$< 10^{-2}$
Tagging	0.03	$< 10^{-3}$	$< 10^{-3}$	$< 10^{-3}$	$< 10^{-3}$	$< 10^{-3}$	0.04	$< 10^{-2}$	$< 10^{-2}$
Acceptance	0.02	0.004	0.002	0.002	0.004	–	–	$< 10^{-2}$	–
Models:									
Default fit	$< 10^{-2}$	0.003	$< 10^{-3}$	0.001	0.001	0.006	0.07	0.01	0.01
Signal mass	$< 10^{-2}$	0.001	$< 10^{-3}$	$< 10^{-3}$	0.001	$< 10^{-3}$	0.03	0.04	0.01
Background mass	$< 10^{-2}$	0.001	0.001	$< 10^{-3}$	$< 10^{-3}$	0.002	0.06	0.02	0.02
Resolution	0.02	$< 10^{-3}$	0.001	0.001	$< 10^{-3}$	0.002	0.04	0.02	0.01
Background time	0.01	0.001	$< 10^{-3}$	0.001	$< 10^{-3}$	0.002	0.01	0.02	0.02
Background angles	0.02	0.008	0.002	0.008	0.009	0.027	0.06	0.07	0.03
Total	0.05	0.010	0.004	0.009	0.012	0.028	0.11	0.09	0.04

Figure 4 shows the contour plots of $\phi_s^{J/\psi\phi}$ vs $\Delta\Gamma_s$ for the untagged 2011 and tagged 2011 data for comparison.

The uncertainty of ϕ_s has improved $\sim$40% since the previous publication [2], and there is now no external constraint placed upon $\delta_\perp$. The $\Delta\Gamma$ central value and uncertainty are unchanged in this analysis within errors. These results are consistent with what has been previously reported in LHCb [3, 4].

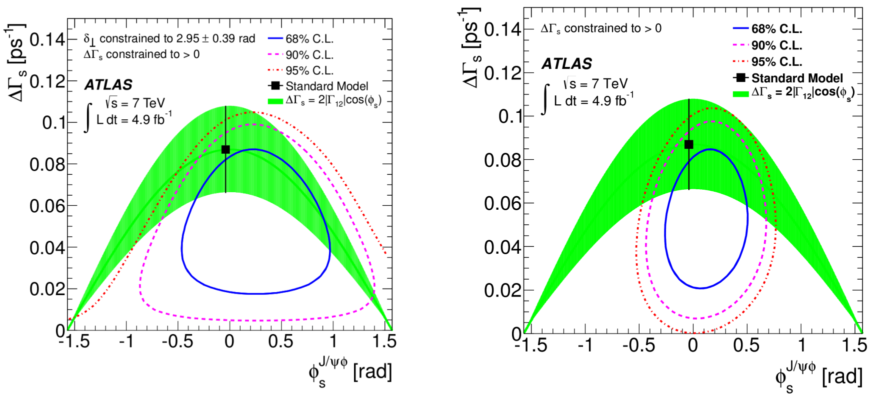

(a) Untagged analysis likelihood contours in $\phi_s - \Delta\Gamma_s$ plane

(b) Tagged analysis likelihood contours in $\phi_s - \Delta\Gamma_s$ plane

Figure 4: Likelihood contours in the $\phi_s - \Delta\Gamma_s$ plane for (a) the untagged 2011 data analysis (taken from [2]) and (b) tagged 2011 data analysis (taken from [1]). The blue lines show the 68% likelihood contour, the dashed pink lines show the 90% likelihood contour and the red dotted lines show the 95% likelihood contour (statistical errors only). The green band is the theoretical prediction of mixing-induced CP violation.

6. Summary

A tagged analysis to extract $B_s^0 \to J/\psi\phi$ decay parameters was performed on 4.9 fb^{-1} of integrated luminosity collected by the ATLAS detector from pp collisions recorded in 2011.

From final results of the maximum likelihood fit performed, the uncertainty of ϕ_s has improved $\sim$40% since the previous publication. There has also been no external constraint placed upon $\delta_\perp$. The extracted $\Delta\Gamma$ central value and uncertainty are unchanged in this analysis within errors, and all results are consistent with world averages [5].

References

[1] The ATLAS Collaboration, *Flavour tagged time dependent angular analysis of the $B_s^0 \to J/\psi\phi$ decay and extraction of $\Delta\Gamma$ and the weak phase ϕ_s in ATLAS*, arXiv:1407.1796.

[2] The ATLAS Collaboration, *Time dependent angular analysis of the $B_s^0 \to J/\psi\phi$ decay and extraction of $\Delta\Gamma$ and the weak phase ϕ_s in ATLAS*, arXiv:1208.0572

[3] The LHCb Collaboration *Measurement of the CP-violating phase ϕ_s in the decay $B_s^0 \to J/\psi\phi$* arXiv:1112.3183

[4] The LHCb Collaboration *Determination of the sign of the decay width difference in the B_s^0 system* arXiv:1202.4717

[5] The Particle Data Group, http://pdg.lbl.gov/